Dimensioning of pillars in stopes

Conventional procedures for calculating pillars in stopes tacitly start from the assumption that the pillars are made of rock material and are subsequently loaded by the weight of the rock up to the ground surface. Based on the total excavation area and the area of the pillars, the corresponding load of each pillar is calculated. In tabular, horizontal deposits at shallow depth, the calculation result corresponds to the real situation. In doing so, the strength of the pillar is the uniaxial compressive strength of the monolith reduced due to the fracturing of the rock mass. The entire calculation procedure is, in fact, a packaging of data so that the result serves as a justification for an empirically designed structure.

In reality, excavation (disintegration) of part of the rock (ore) is carried out in a stressed rock mass, and the consequence is the created underground opening (stope). If the excavation method implies that the opening must be stable, then the shape and dimensions of the underground opening should be adjusted to the strength of the rock and its stress state.

If we consider a horizontal tabular deposit whose width (length) is many times greater than the stable width of a single excavation drift (opening), then a larger number of parallel excavation drifts can be placed in the deposit. The unexcavated part of the rock (ore) between two drifts is a safety pillar. The part of the ore that remains in the safety pillar is most often a permanent loss, so there is a reasonable tendency to make the pillar as small as possible. The procedure of determining the minimum safe distance between two excavations is called the dimensioning of the safety pillar.

If the two excavation drifts that form the safety pillar are stable, then the pillar will also be stable. Therefore, the entire stope and all excavation drifts within it, and all pillars between them, will be stable if the excavation drifts are made stable by their dimensions, geometric shape, and possibly by support construction.

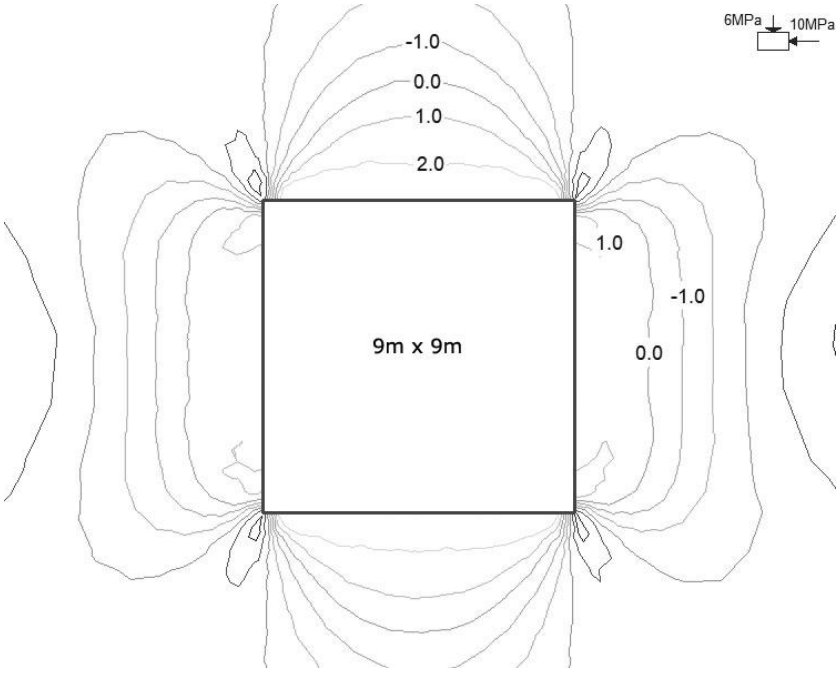

Figure 1. Tensile zones around a single drift

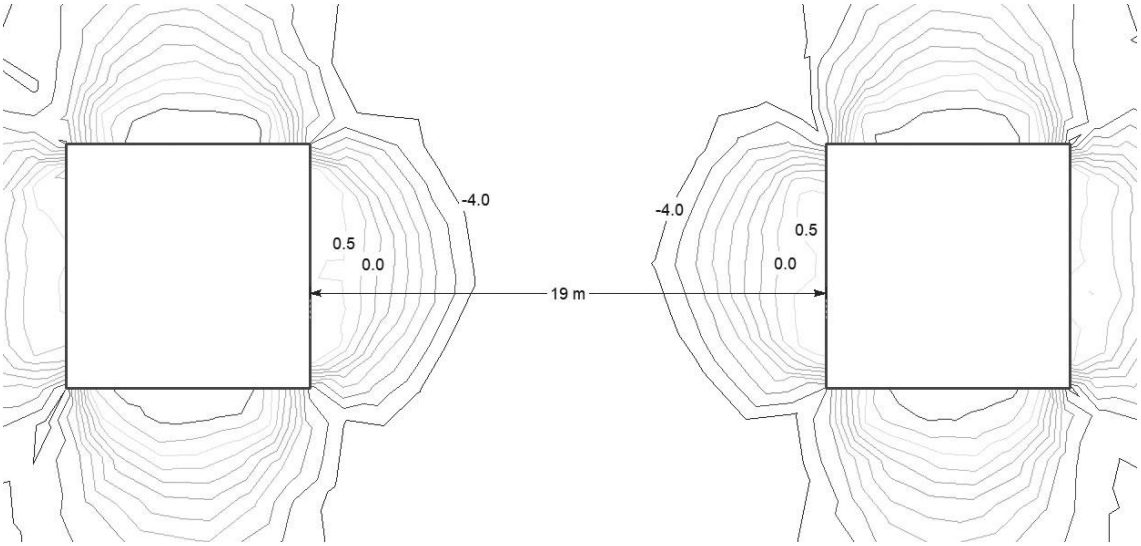

Figure 2. Tensile zones around two parallel drifts at a distance of 19 m

Demonstration of the correctness of the approach

In a rock mass with a primary stress state defined by a vertical stress $\sigma_v = 6MPa$ and a maximum horizontal stress $\sigma_H = 10MPa$, a drift with dimensions 9m × 9m was excavated. A stress–strain analysis was performed using the finite element method, and Figure 1 shows the tensile zone within the "0" isoline. Negative values indicate compressive stress. Although not shown in Figure 1, an influence zone of the excavated opening was identified up to the 19th meter from the edge of the opening. For this reason, another opening of the same dimensions was modeled at a horizontal distance of 19m. The calculation result is shown in Figure 2. It is evident that these two openings do not have a significant influence on each other. Attention is paid only to the space between the two openings. There is no change in the shape or size of the tensile zone. In the next step, the distance between the excavation drifts was reduced to 13m, Figure 3. An interaction between the two openings is evident. The stress distribution, i.e. the induced stresses on the side where the second excavation exists and on the opposite side, is significantly different. In this case, the part of the rock mass between the two excavation drifts can be designated as a "pillar". The tensile stress zone is significantly larger, and the maximum tensile stress on the sides of the underground openings is also increased. The next step in this experiment is reducing the distance to 9 m, Figure 4. In this case, it is observed that the tensile zones of the individual drifts have merged into a common zone that occupies the center of the pillar, with a further increase in the maximum tensile stress on the sides of the openings.

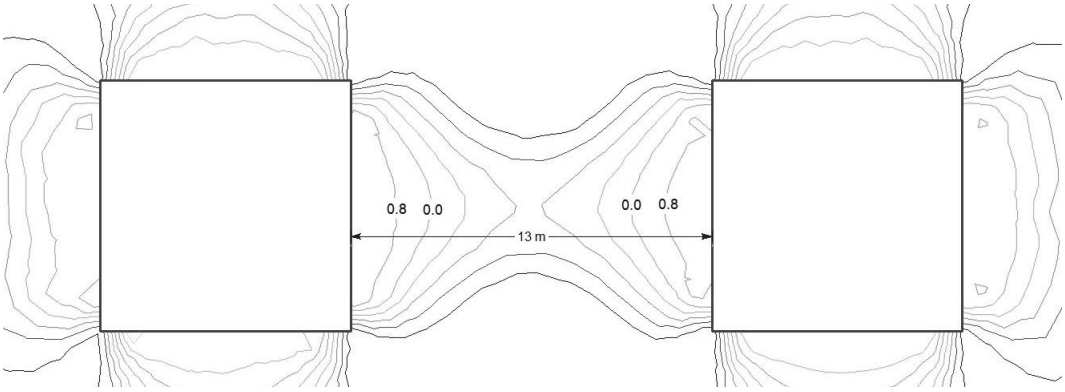

Figure 3. Tensile zones around two parallel drifts at a distance of 13m

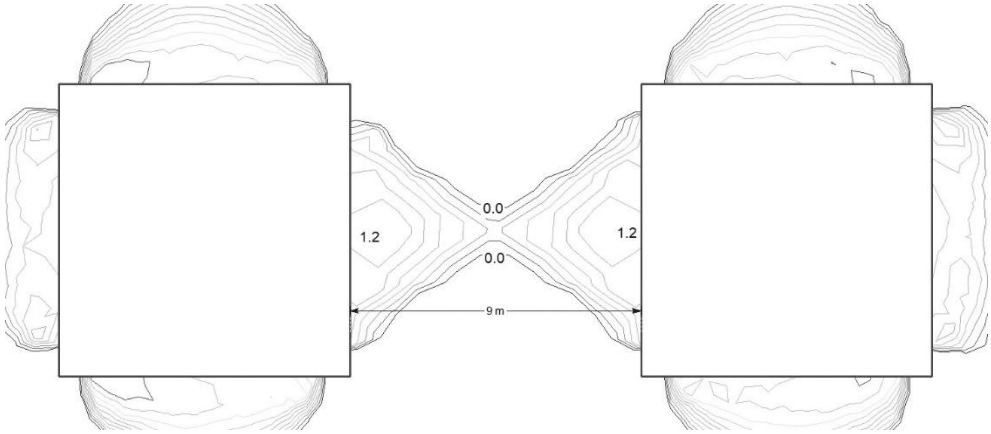

Figure 4. Tensile zones around two parallel drifts at a distance of 9m

The next series of experiments was carried out for two excavation chambers with a width of 9m and a height of 27m, while the width of the pillar between the chambers was varied. The first experiment was with a pillar width of 9m, Figure 5. As before, the size of the zone and the intensity of tensile stress in the pillar between the chambers were monitored. It is noticeable that the entire pillar is subjected to tension and that the intensity of tensile stress is from 2.1 MPa to 2.3 MPa. Pillar widths of 7 m, 5 m, and 3 m were also modeled, with all other dimensions of the structure unchanged. It is evident that the same level of tensile stress occurs in the protective pillar. The difference in tensile stress between a pillar 9 m wide and a pillar 3 m wide is only 0.2 MPa. It is clear that tensile stress, which causes failure, is not influenced by the pillar width but by the width of the excavation chambers that form the pillar.

The next series of experiments was performed using the final model from the previous series. That is, the first model in this series has two chambers 9 m wide, with a pillar width of 3 m between them. The height of the chambers, i.e. the height of the pillar, was reduced from 27 m to 22 m, Figure 9. The tensile stress at the center of the pillar increased to 1.4 MPa. Then experiments were carried out with chamber heights of 18 m, Figure 10; 9 m, Figure 11; and 5 m, Figure 12. The reduction of chamber height is accompanied by an increase in tensile stress at the center of the pillar. Thus, for a chamber (pillar) height of 5 m, the tensile stress in the safety pillar is 3 MPa. It is evident that the tensile stress is also influenced by the height of the excavation chambers that form the pillar.

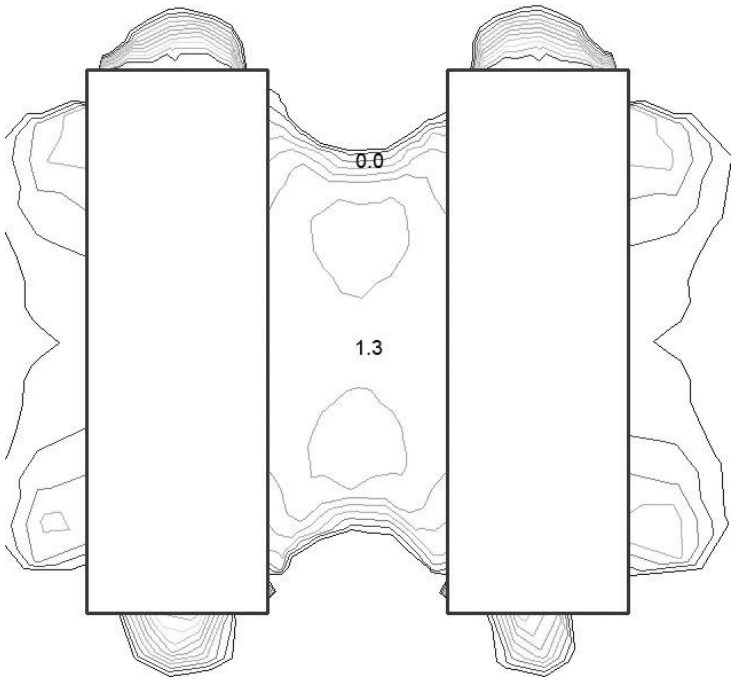

Figure 5. Tensile zones around two parallel excavations 9 m wide, 27 m high, at a distance of 9 m

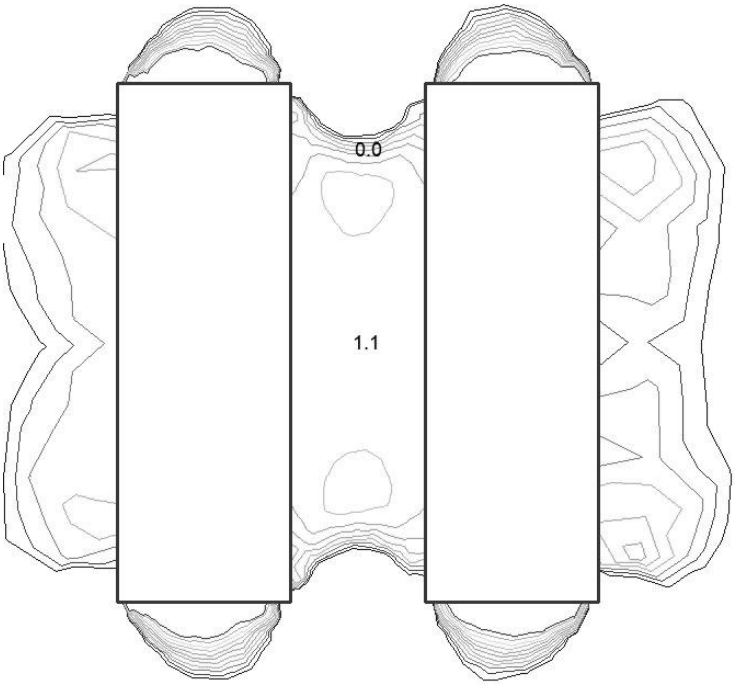

Figure 6. Tensile zones around two parallel excavations 9 m wide, 27 m high, at a distance of 7 m

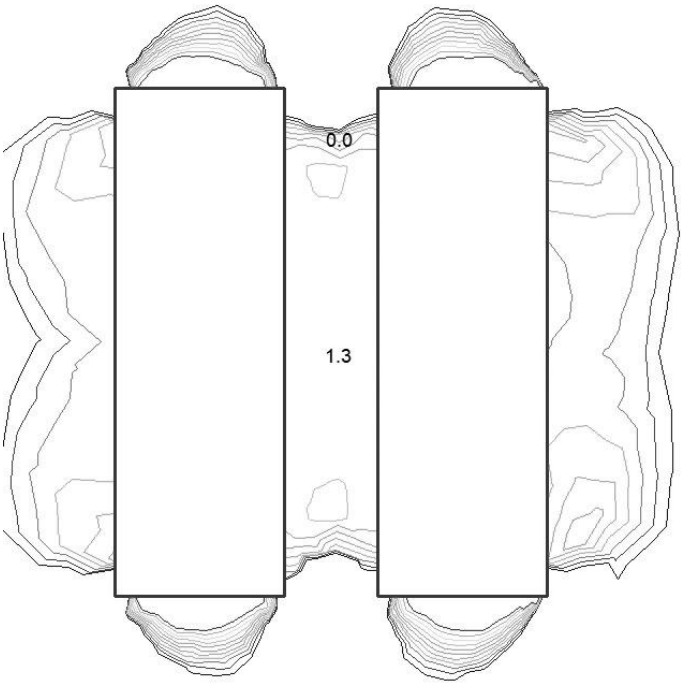

Figure 7. Tensile zones around two parallel excavations 9 m wide, 27 m high, at a distance of 5 m

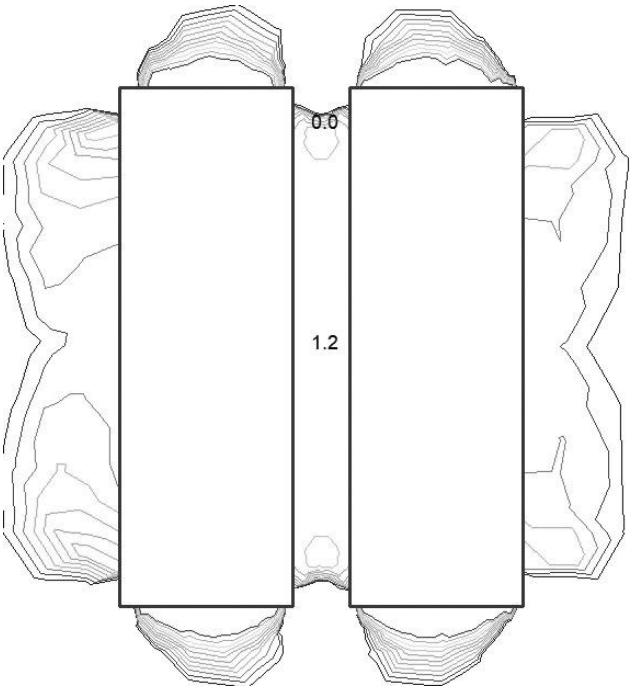

Figure 8. Tensile zones around two parallel excavations 9 m wide, 27 m high, at a distance of 3 m

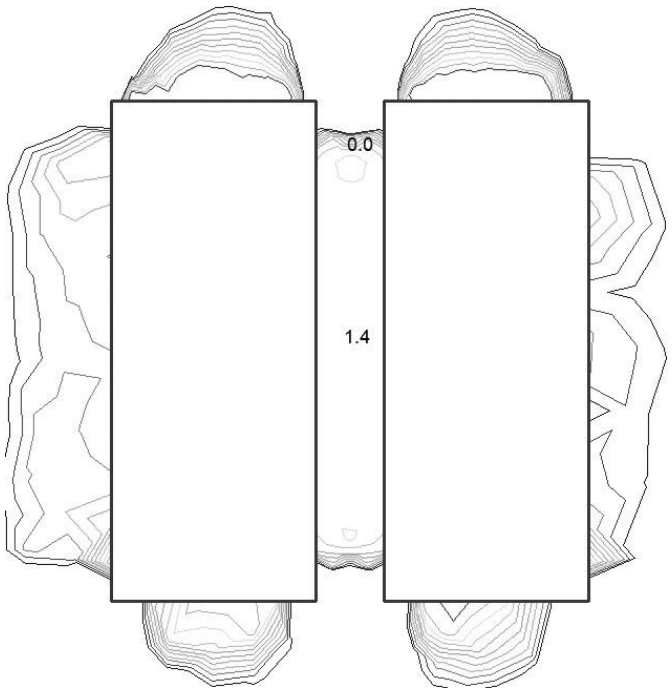

Figure 9. Tensile zones around two parallel excavations 9 m wide, 22 m high, at a distance of 3 m

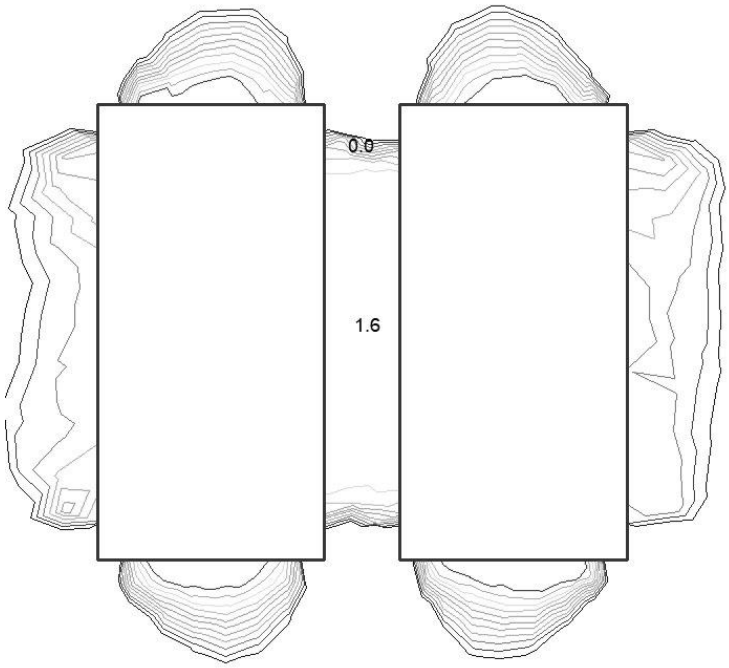

Figure 10. Tensile zones around two parallel excavations 9 m wide, 18 m high, at a distance of 3 m

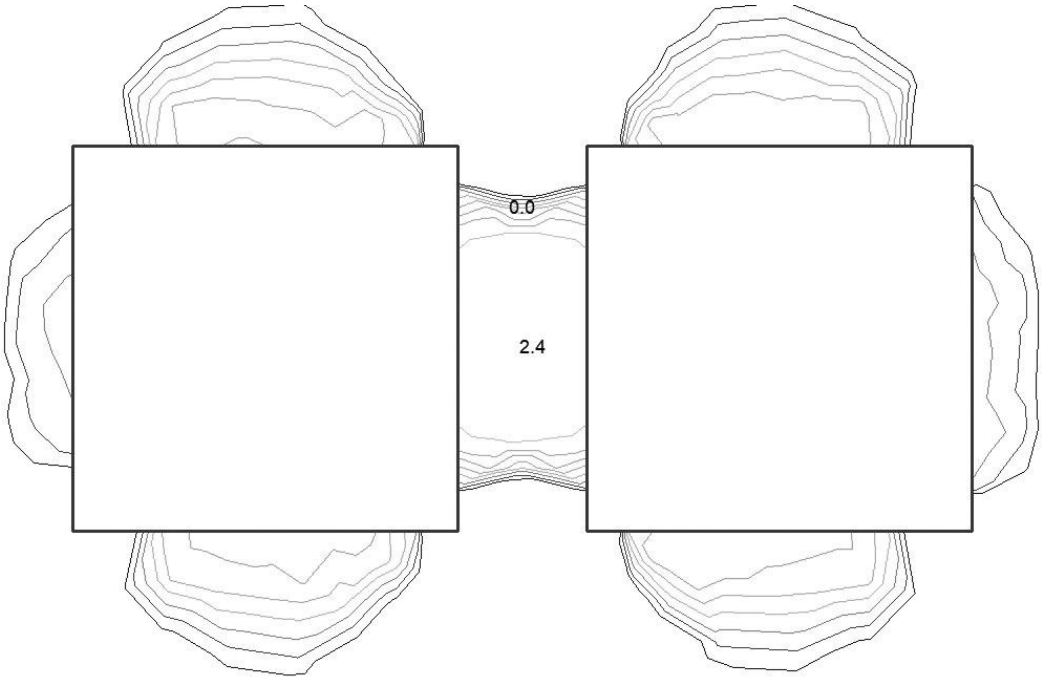

Figure 11. Tensile zones around two parallel excavations 9 m wide, 9 m high, at a distance of 3 m

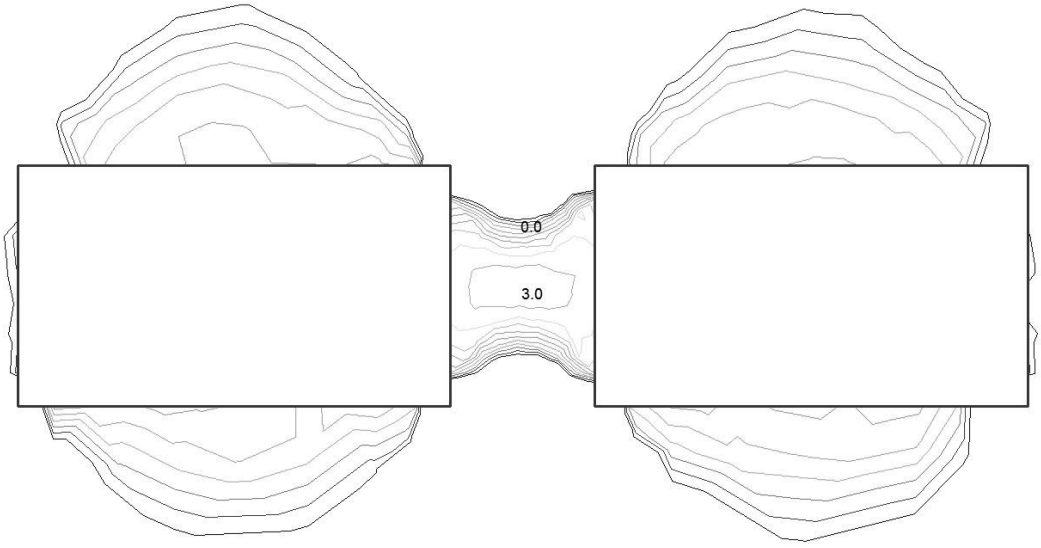

Figure 12. Tensile zones around two parallel excavations 9 m wide, 5 m high, at a distance of 3 m

If we return to the model in Figure 4, in which a 9 m × 9 m pillar is formed by two chambers of the same dimensions 9 m × 9 m, we observe a tensile zone that narrows from the periphery toward the center of the pillar. When the sides of the chambers that form the pillar are rounded, Figure 13, the cross-section

of the pillar takes on an hourglass shape, and the tensile stress disappears from the core of the pillar. The stress zone exists only along the side of the excavation chamber, and the stress intensity decreases with distance from the side.

Those who have not had the opportunity to see this in an underground stope can find many photographs of this phenomenon on the internet. These pillars were originally primarily with vertical sides, and the observed shape arose spontaneously. Failure begins at half the height of the pillar when the tensile stress exceeds the failure limit, i.e. the allowable tensile strength. The failure stops when the system equilibrates, that is, when the condition is satisfied that:

$$\sigma_{td} + \sigma_3 = st \cdot \sigma_1$$

Figure 14 shows the directions of the principal stresses and their intensities for both excavation chamber structures.

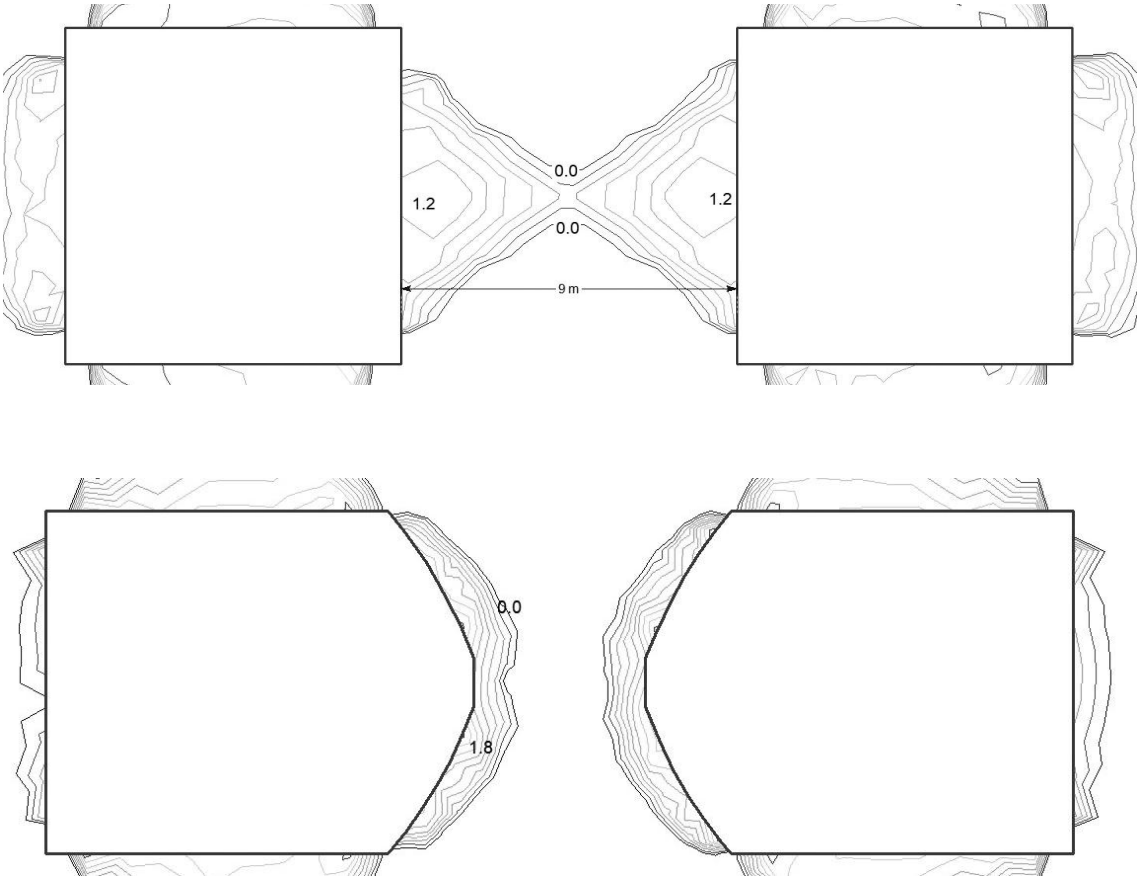

Figure 13. Influence of structural shape on the shape and size of the tensile zone and the intensity of tensile stress

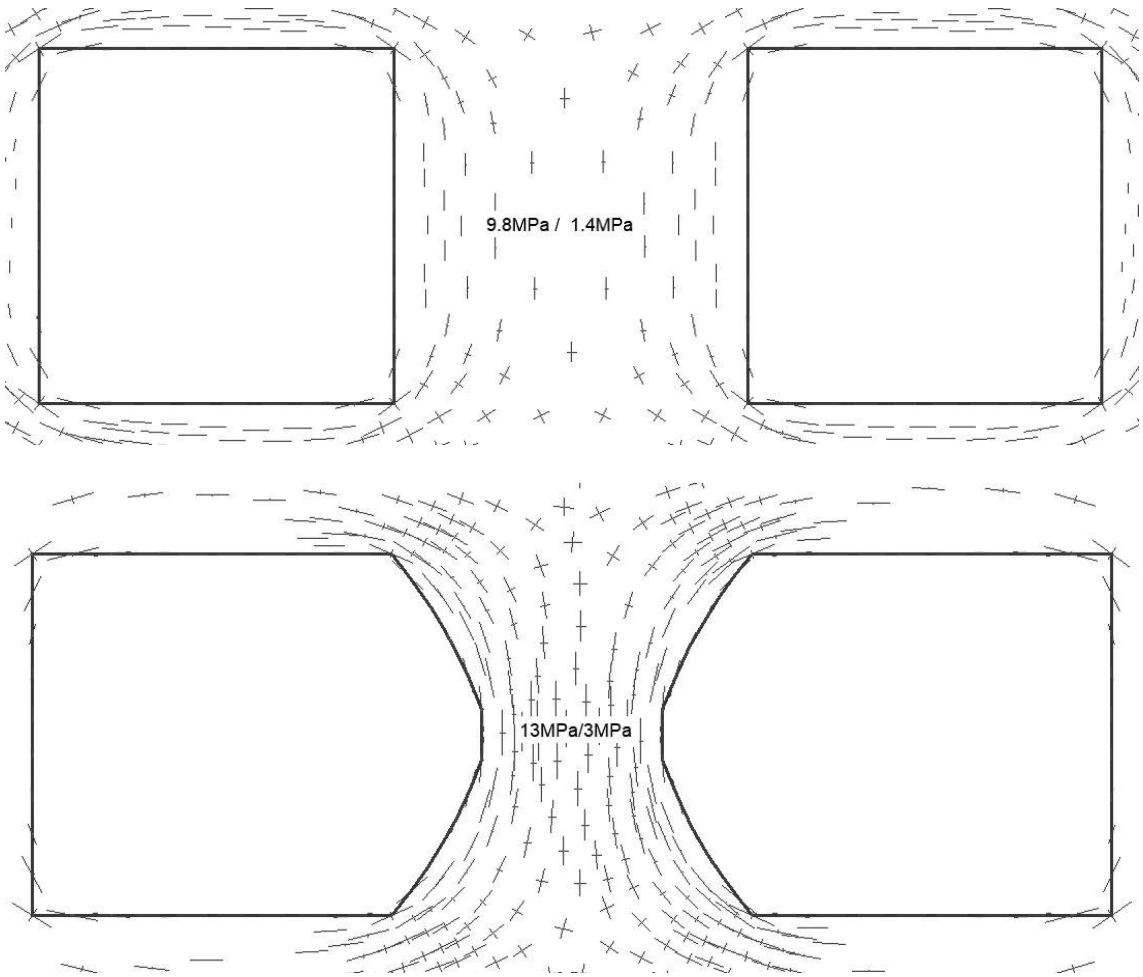

Figure 14. Influence of structural shape on the intensity of maximum and minimum principal stresses

As previously explained, the shape of the structure affects its resistance. The tensile stress on the sides of the underground opening is:

$$\sigma_t = st \cdot \sigma_1 - \sigma_3$$

In this case, the considered pillar is the common side of two adjacent excavation openings. The tensile coefficient is:

$$st = \frac{\nu}{1 + tg\varphi} = \frac{0{,}3}{1 + tg35^{\circ}} = 0.176$$

Thus, in the first case with a flat side wall of the excavation (pillar), the tensile stress at the center of the pillar is:

$$\sigma_t = 0{,}176 \cdot 9.8 - 1{,}4 = 0{,}325MPa$$

And when the sides of that pillar are adjusted to approximately follow the isolines of tensile stress, the tensile stress at the center of the pillar is:

$$\sigma_t = 0{,}176 \cdot 13 - 3 = -0{,}73MPa$$

The negative value indicates that the center of the pillar is not subjected to tension but to compression.

Strip and square pillars

All previous models and analyses were performed using the finite element method under plane strain conditions. The graphical representations show cross-sections of the pillars, while their length is undefined. Such pillars are called strip pillars, Figure 15.

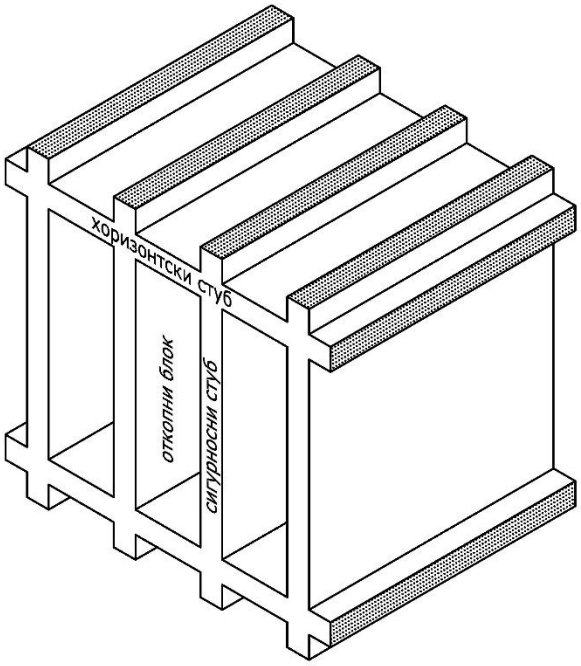

Figure 15. Example of strip pillars between excavation chambers

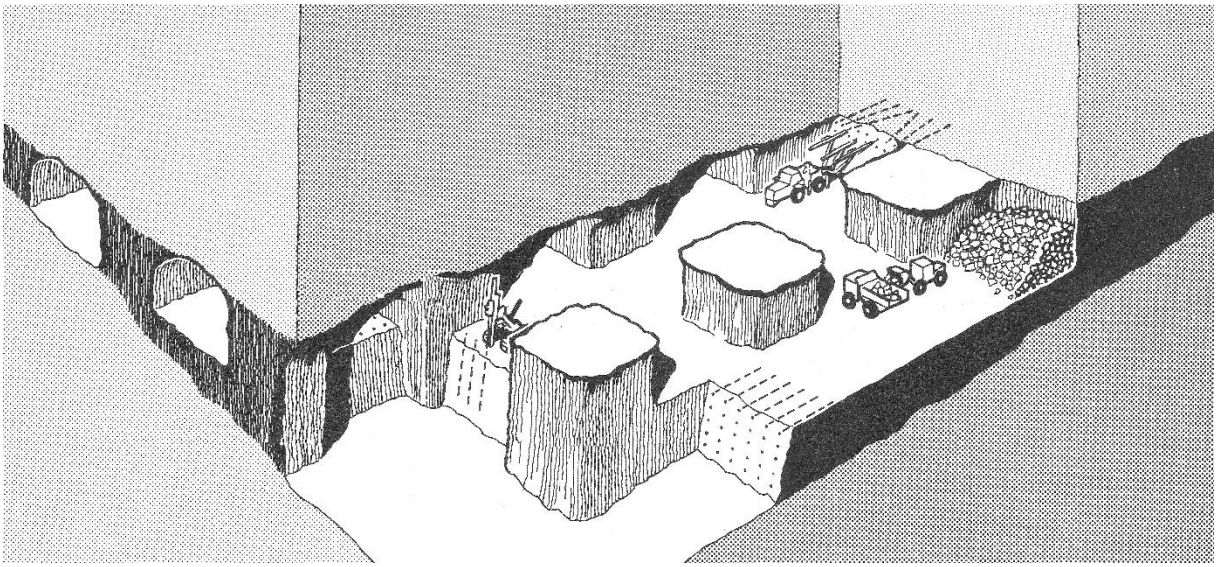

Figure 16. Example of square pillars in a stope

In a number of other excavation methods, square safety pillars are left in the stope, Figure 16. The cross-section of such an excavation does not satisfy the basic condition for plane strain, which complicates matters in the generally accepted approach to pillar calculation.

However, as already shown, an excavated underground opening is a source of disturbance to the existing equilibrium. Deformation work, i.e. the movement of particles toward the empty space, is performed at the expense of the potential energy of the elastically deformed rock that constitutes the pillar. Potential energy and the corresponding deformation work are associated with each particle. Accordingly, a particle can move in accordance with the energy it possesses and the resistance to movement, which is a characteristic of the material and the position of the particle relative to other particles with which it is in contact, which is a characteristic of the structure.

The shape and size of the opening condition the redistribution of the components of the rock stress state. If the analyzed strip pillar is divided into a series of prisms with a square base, square pillars can be formed by removing the prisms between them and converting that space into excavation chambers. This will result in additional deformation work at the expense of the stress component perpendicular to the newly formed surface. If both components of the horizontal stresses of the rock mass are the same and if the widths of the excavation chambers are the same, then the deformation in this direction will be the same as in the direction perpendicular to it.

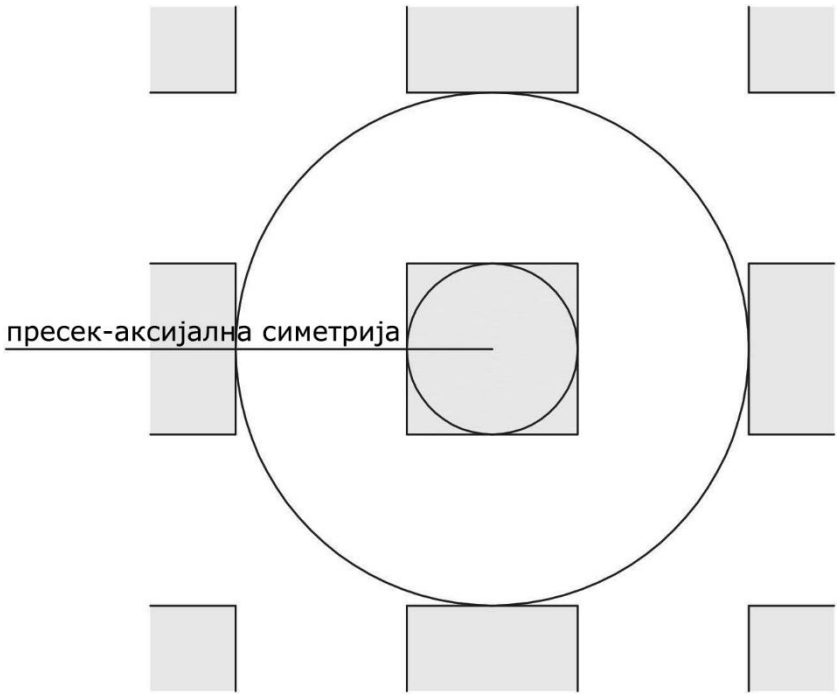

Figure 17. Modeled pillar and excavations with the position of the section for an axially symmetric model

This means that the stability calculation of a strip safety pillar is simultaneously the stability calculation of a square safety pillar for the same widths of the excavation drifts (chambers) that form it. Since the components of horizontal stresses are not the same, the maximum horizontal stresses will be used as the governing ones for the calculation.

This assertion will be supported by the following proof. On the excavation plan with a square pillar and excavation drifts (chambers) that form it and directly influence its stability, we located the position of the section for an axially symmetric model of the structure. In this case, the square pillar is modeled as a circular one, and the empty space (excavation) is an annular opening with the same cross-sectional area. A graphical representation of the distribution of the tensile stress zone and the stress intensities for both models is shown in Figure 18. The size and appearance of the stress zone are identical in both models. In the axially symmetric model, the values of tensile stress are somewhat lower. The reason for this is that the outer wall of the chamber in the model has a circular shape (instead of square), and therefore the structural resistance is greater, as previously explained.

For now, the question remains open as to what the minimum rational dimension of a safety pillar is, given that the stress in the pillar does not depend on the dimensions of the pillar but on the dimensions and shape of the chambers that form the pillar.

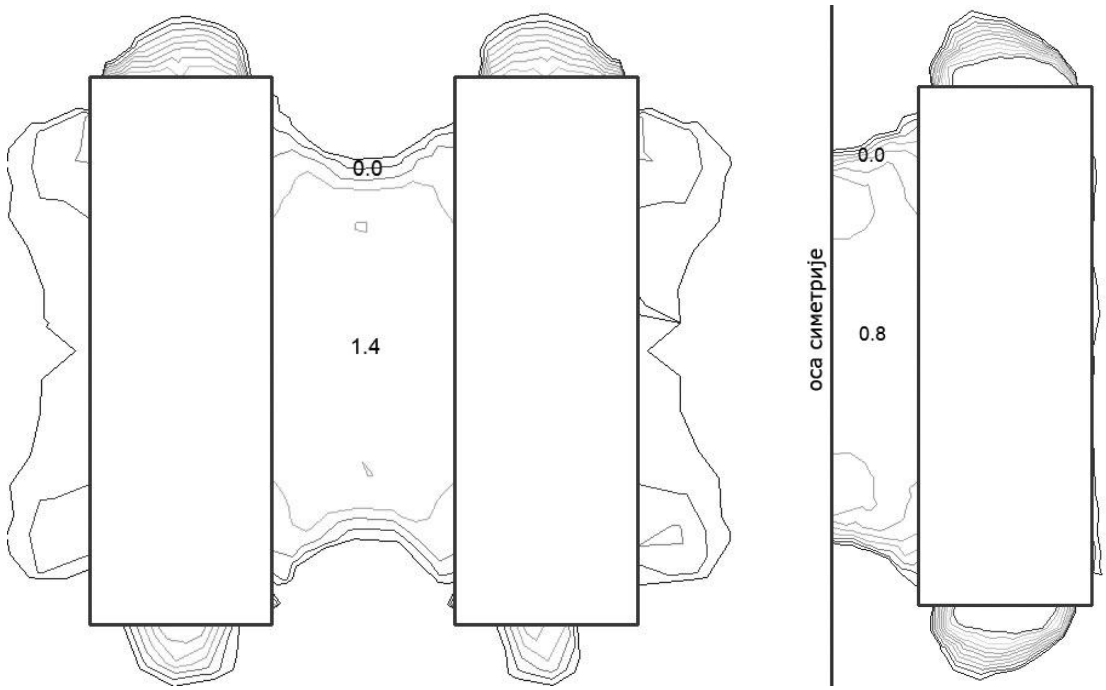

Figure 18. Comparative presentation of the tensile stress state in the pillar for plane strain and axial symmetry conditions

Safety factor

The procedure of dimensioning a structure подразумева adjusting its dimensions and shape so that the stress that causes failure is aligned with the strength of the material. Since failure is caused by tensile stress, the equilibrium condition is:

$$\sigma_{td} + \sigma_3 = st \cdot \sigma_1$$

The allowable tensile stress (σ_{td}) is the measured tensile strength (σ_{ti}) increased by the safety factor (k_s):

$$\sigma_{td} = \frac{\sigma_{ti}}{k_s}$$

Safety factors in engineering practice range from several tens to several hundreds of percent. This depends on the reliability of the calculation method and the reliability of the input data used in the calculation.

In this case, I propose that the safety factor be determined as a function of the Geological Strength Index of the rock mass (GSI):

$$k_s = 2 - \frac{GSI}{100}$$